Active Properties of Neocortical Pyramidal Neuron Dendrites

3 authors:

Guy Major
Cardiff University
27 PUBLICATIONS   **2,212** CITATIONS

SEE PROFILE

Matthew E Larkum
Humboldt-Universität zu Berlin
137 PUBLICATIONS   **10,595** CITATIONS

SEE PROFILE

Jackie Schiller
Technion - Israel Institute of Technology
81 PUBLICATIONS   **7,387** CITATIONS

SEE PROFILE

Some of the authors of this publication are also working on these related projects:

Feedforward motor information enhances somatosensory responses and sharpens angular tuning of rat S1 barrel cortex neurons View project

Air-track View project

Active Properties of Neocortical Pyramidal Neuron Dendrites

Guy Major,[1] Matthew E. Larkum,[2,*]
and Jackie Schiller[3,*]

[1]School of Biosciences, Cardiff University, Cardiff, CF10 3AX, United Kingdom;
email: majorg@cardiff.ac.uk

[2]Charité University, Neuroscience Research Center (NWFZ), D-10117 Berlin, Germany;
email: matthew.larkum@gmail.com

[3]Department of Physiology, Technion Medical School, Haifa 31096, Israel;
email: jackie@techunix.technion.ac.il

*These authors contributed equally to this work.

Keywords

spike, action potential, NMDA receptor, NMDAR, synaptic
integration, computational subunit

Abstract

Dendrites are the main recipients of synaptic inputs and are important
sites that determine neurons' input-output functions. This review fo-
cuses on thin neocortical dendrites, which receive the vast majority of
synaptic inputs in cortex but also have specialized electrogenic prop-
erties. We present a simplified working-model biophysical scheme of
pyramidal neurons that attempts to capture the essence of their dendritic
function, including the ability to behave under plausible conditions as
dynamic computational subunits. We emphasize the electrogenic ca-
pabilities of NMDA receptors (NMDARs) because these transmitter-
gated channels seem to provide the major nonlinear depolarizing drive
in thin dendrites, even allowing full-blown NMDA spikes. We show
how apparent discrepancies in experimental findings can be reconciled
and discuss the current status of dendritic spikes in vivo; a dominant
NMDAR contribution would indicate that the input-output relations
of thin dendrites are dynamically set by network activity and cannot be
fully predicted by purely reductionist approaches.

Contents

CURRENT OVERALL UNDERSTANDING OF THE NEOCORTICAL PYRAMIDAL NEURON

The layer 5 pyramidal neuron is the largest neuron of the cerebral cortex, extending its dendrites for more than 1 mm across the cortical layers. This review assesses our knowledge of this important cell type and of other neocortical pyramidal neurons, in terms of the electrical properties and information-processing capabilities of their dendrites (first and second sections). We also provide a framework for understanding the role of dendrites in the cortical network (third and fourth sections). The complex and strikingly beautiful shape of a pyramidal neuron is a fundamental determinant of signal flow within it (Larkman et al. 1992, Rapp et al. 1996, Rhodes & Llinas 2001, Spruston et al. 1994, Stafstrom et al. 1984), as well as the pattern and types of synaptic input it can receive (Cauller & Connors 1994, Dantzker & Callaway 2000, Larkman 1991, Petreanu et al. 2009). However, the active properties of dendrites also have a profound influence (Johnston et al. 1996, Mel 1993, Migliore & Shepherd 2002, Rhodes 1999, Spruston 2008). Understanding the transformation of synaptic inputs to output action potentials (APs) is therefore an incredibly complex task involving the combination of input patterning, dendritic architecture, signal transformation, and regenerative properties.

Dendrites Under the Linear Regime

EPSP size: location-dependent somatic impact of single synaptic inputs. The first major question concerns the impact of the passive dendritic architecture on the size and spread of electrical signals impinging on different portions of the basal, oblique, and tuft trees (Agmon-Snir & Segev 1993, Gulledge et al. 2005, Larkman et al. 1992, Magee 2000, Major et al. 1994, Mel 1994, Stuart & Spruston 1998, Williams & Stuart 2003). Direct patch pipette recordings of miniature excitatory

postsynaptic potentials (EPSPs) in basal, apical trunk, and tuft dendrites reveal that distal basal, apical, and tuft EPSP peak voltages attenuate similarly, by ∼30-fold or more, as they spread from the synapse to the closest downstream (more proximal) intrinsic spike initiation zone (**Figure 1**), either at the soma/axon initial segment or around the main apical bifurcation point (Larkum et al. 2009, Nevian et al. 2007, Williams & Stuart 2002). In contrast to the strong attenuation of peak voltage, the loss of current along the input dendrite itself is comparatively minor (Agmon-Snir & Segev 1993, Williams 2004), reflecting the fact that its membrane resistance is around an order of magnitude higher than its axial resistance over much of the likely biological parameter range.[1] In the case of basal and oblique branches, whatever the synapse site, most of the charge injected flows rapidly via the soma to the rest of the cell's membrane capacitance before more slowly leaking out through the membrane resistance; over the distal ∼80% of these trees, input location per se makes only a relatively minor contribution to variations in postsynaptic potential (PSP) amplitude at the soma (Hardingham et al. 2010, Stratford et al. 1989).

Dendritic integration. Dendritic integration (how dendritic inputs combine to influence the membrane potential) has been extensively reviewed (Rall 1977, Stuart et al. 1999). One school of thought is that passive/linear or sublinear summation is the dominant mode of neocortical dendritic integration (Cash & Yuste 1999, Priebe & Ferster 2010). This would be more likely if inputs are activated in a distributed and sparse manner onto the dendritic tree (Jia et al. 2010, Varga et al. 2011) (see third section, below). The result is an "every input for itself," non-cooperative type of integration; the final input-output transformation is dominated by the passive properties of the dendritic tree

(although linear summation is not synonymous with passive behavior).

Passive summation is far from boring or trivial. For example, PSP rise times at the soma differ as they spread from different locations in the dendritic tree (Agmon-Snir & Segev 1993, Major et al. 1994, Rinzel & Rall 1974). This could be exploited for computing the direction of input sequences lasting within the proximal-to-distal range of EPSP rise times (Rall 1964). Because their peaks coincide, distal-to-proximal sequences of synaptic inputs will result in a larger voltage surge at the soma than would the same inputs in reverse order. I_h (hyperpolarization-activated conductance) in the distal apical trunk and tuft may selectively reduce the duration of PSPs originating from these branches, while having much less effect on basal dendritic PSPs (Berger et al. 2001, Berger & Lüscher 2003, Kole et al. 2006, Williams & Stuart 2000).

Regenerative Mechanisms and Spikes in Dendrites

Both in vitro recordings and modeling studies have shown that dendrites can switch to a highly supralinear regime, which in principle can lead to so-called dendritic spikes (Ariav et al. 2003, Häusser et al. 2000, Judkewitz et al. 2006, Larkum & Nevian 2008, Losonczy & Magee 2006, Mel 1993, Polsky et al. 2004, Rhodes 2006, Schiller et al. 1997, Schiller & Schiller 2001, Spruston 2008). Do pyramidal cell dendrites actually fire spikes? Are voltage-sensitive channels in dendrites activated in an all-or-none manner during normal brain function, or do they simply boost synaptic inputs in a graded fashion? What does all-or-none actually mean (see sidebar, Terms)? This topic remains contentious despite decades of evidence suggesting the existence of all-or-none dendritic events under certain conditions (Amitai et al. 1993, Llinás et al. 1968, Schiller et al. 1997, Schwindt & Crill 1997, Stuart & Sakmann 1994, Wong et al. 1979, Yuste et al. 1994, Xu et al. 2012). The question is perhaps better restated as whether we should expect

---

[1] During the awake state or network upstates, however, membrane conductance and hence current loss may increase several-fold.
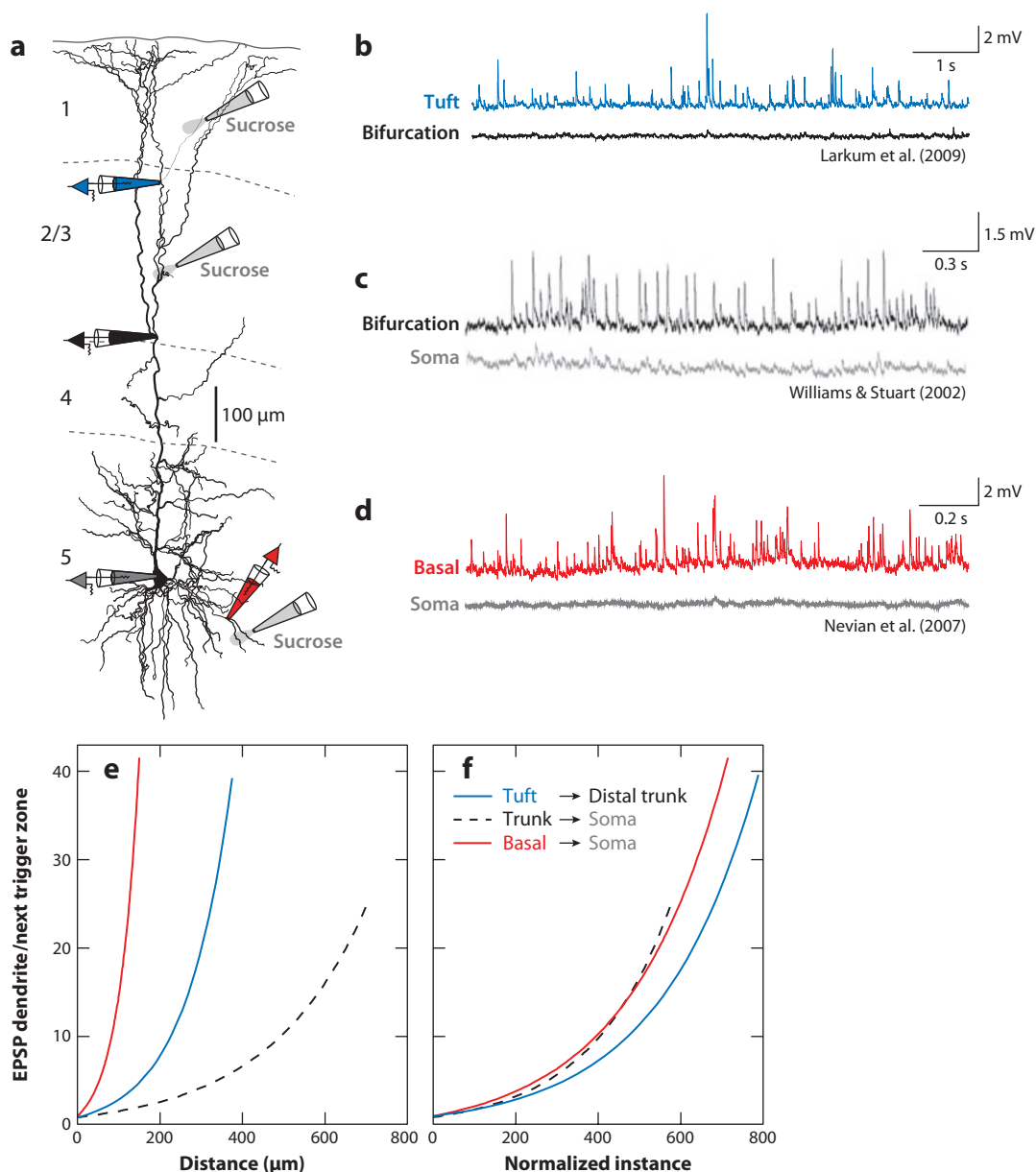
Figure 1

Attenuation of miniature excitatory postsynaptic potentials (mEPSPs) across the dendritic tree. (*a*) Sucrose-evoked mEPSPs at different locations in the L5 pyramidal neuron. Whether evoked in the distal tuft and recorded (*b*), or evoked near the apical bifurcation and recorded at the soma (*c*), or evoked in the basal dendrites and recorded at the soma (*d*), most individual propagated mEPSPs were barely detectable: in terms of attenuation, the two spike trigger zones (both the calcium initiation zone near the apical bifurcation and the sodium initiation zone near the soma) appear electrically remote from the sites distal to them providing the bulk of their synaptic input. (*e*) Attenuation of EPSPs across different regions of the dendritic tree (peak V near synapse/peak V near next downstream spike trigger zone). (*f*) Distances normalized to average total length of the respective dendrites.

dendrites to spike under relevant physiological conditions. We argue here that this question can be approached in principle in terms of the net current-voltage (I-V) relationships of dendritic compartments. In this context, many of the currently confusing and disparate results can easily be reconciled into a unified framework. We do not attempt to archive exhaustively all the details of active dendritic properties in neocortical pyramidal neurons, which have been addressed in several other reviews (London & Häusser 2005, Migliore & Shepherd 2002, Spruston 2008).

One dominant ion? Not necessarily. The word spike has been a convenient term for most of the history of neuroscience, typically being used to denote the firing of a sodium AP, usually recorded at the soma but actually arising in the axon (Kole & Stuart 2008, Stuart et al. 1997). The discovery that dendrites are capable of electrogenesis (Amitai et al. 1993, Llinás et al. 1968, Wong et al. 1979) undermined this once simply understood terminology. Although all dendritic spikes are somewhat mixed in nature, one can differentiate between three major types of spikes—Na^+, Ca^{2+}, and N-methyl-D-aspartate (NMDA)—according to the main underlying class of conductance. The wide range of electrical properties, channel types, and densities gives rise to regenerative events in dendrites whose rise times and durations differ by orders of magnitude. Nonetheless, dendritic spikes do conform to the classical description of APs in as much as they have a threshold, and some types have a refractory period and propagate actively for some distance (Larkum & Zhu 2002, Schiller et al. 1997).

All-or-none? Yes. Stereotyped? No. The term all-or-none is also a source of much confusion: Even classical Na^+ APs are far from stereotyped in threshold, amplitude, and time course. No feature is sacred: All three change during the relative refractory period, with strength-duration and strength-length trade-offs, and all three depend on the rate of rise of the stimulus (Azouz & Gray 2000, de Polavieja

TERMS

These only partially overlap and are not synonymous.

Regenerative event: a self-driven event (waveform) involving a positive feedback loop, e.g., between voltage and current (or calcium and voltage, or calcium-induced calcium release).

Spike: a voltage transient; in the wider world, many shapes and sizes; generally agreed it must go up then down (or vice versa, i.e. be self-terminating). In neuroscience, by convention, a spike usually has a threshold of some kind across which the response jumps qualitatively/substantially in size/shape, in a biologically/computationally significant manner. Threshold can be voltage or an input variable such as glutamate, or indeed it can be multidimensional. Threshold does not need to be fixed (e.g., strength-duration trade-offs, relative refractory periods) and may need to be teased out: It may not be apparent in all input-output (I-O) relations, even though the voltage waveform is spike-like and very similar to a supra-threshold waveform from another I-O relation that does exhibit a clear threshold (see section on Sharpness of Threshold and Spike-Sigmoid Duality below).

Action potential (AP): a membrane-voltage transient that normally results in some distinct biological action (e.g., a muscle contraction or release of neurotransmitter); usually, but not necessarily, all-or-none. The term action potential has a broader meaning than many neuroscientists may assume: for example, cardiac action potential = slow spike + plateau; *Nitella* (algae) chloride-mediated action potential; negative-going action potentials in *Ascaris* (roundworm) pharyngeal muscle (Byerly & Masuda 1979).

All-or-none: an event that, once started (i.e., by some threshold being exceeded), proceeds by itself to completion; if not started (i.e., threshold not reached), a substantially different (smaller/briefer) event results. However, all-or-none does not mean completely stereotyped in size and shape (or threshold).

Electrogenic: causing an electrical change. Includes positive feedback, negative feedback (such as sag, undershoot, afterhyperpolarizations), and delayed combinations of the two (e.g., oscillations, pacemaking).

et al. 2005, McCormick et al. 2007, Platkiewicz & Brette 2011, Shu et al. 2006, Tateno et al. 2004, Wilent & Contreras 2005, Yu et al. 2008). Typically, during an AP train, amplitude decreases, duration increases, and threshold

rises (Spruston et al. 1995b). This progression is very marked during high-frequency bursts: Changes in amplitude or duration can be as much as twofold, owing to Na^+ channel inactivation, Ca^{2+} accumulation, and the opening of calcium-activated potassium channels ($gK_{Ca}s$) (Storm 1990). Neuromodulation and inhibition can produce additional changes. So, the term all-or-none does not imply a completely stereotyped waveform; it implies only the existence of some instantaneous threshold below which the response is small and above which the response is clearly bigger, or substantially different (see sidebar, Terms). A similar contention arises over whether dendritic spikes are actually sharply spike-like in shape. In particular, Ca^{2+} spikes and NMDA spikes are often plateau-shaped and are referred to as such (Antic et al. 2010, Milojkovic et al. 2007, Schwindt & Crill 1999, Suzuki et al. 2008, Wei et al. 2001). Considering the biological literature as a whole, APs do not have to be fast: cardiac APs can be hundreds of milliseconds long.

The NMDA spike as a hallmark of electrogenesis in thin dendrites. A consensus is emerging that in neocortical excitatory neurons the dominant depolarization-activated conductance in thin (usually submicron-diameter) dendrites is the NMDA receptor (NMDAR) channel (Antic et al. 2010, Branco & Häusser 2011, Larkum et al. 2009, Lavzin et al. 2012, Major et al. 2008, Mel 1993, Nevian et al. 2007, Schiller et al. 2000). NMDA spikes represent an important conceptual leap because they are inherently ligand dependent, i.e. dependent on glutamate and D-serine binding, and therefore subject not just to local membrane potential but also to the spatial distribution of these transmitters along the dendrite. The clear existence of NMDA spikes in vitro, with an order-of-magnitude safety factor, demonstrates that the input-output relations of thin dendrites are neither fully predictable nor constrainable in a purely bottom-up, reductionist manner.

In vitro, NMDA spikes (or plateau potentials) have been found in all classes of thin dendrite of neocortical excitatory neurons (basals,

apical obliques, apical tufts) and in all neocortical areas and layers examined to date (Branco & Häusser 2011, Gordon et al. 2006, Lavzin et al. 2012, Milojkovic et al. 2004, Nevian et al. 2007, Schiller et al. 2000). They also probably occur in hippocampal apical tufts (Wei et al. 2001). Sodium spikelets, however, are much more difficult to initiate in neocortical pyramidal neuron thin dendrites in brain slices, and are weak and variable in size, if they can be triggered at all (Larkum et al. 2009, Milojkovic et al. 2005b, Nevian et al. 2007). In vitro, calcium spikes are not evoked in basal dendrites either by direct current injection or by glutamate stimulation (Major et al. 2008, Nevian et al. 2007, Schiller et al. 2000); Ca^{2+} spikes are rarely initiated by current injection into single distal (thin) tuft dendrites (Larkum et al. 2009), although most of the depolarization from Ca^{2+} spikes initiated in the distal trunk/bifurcation zone does propagate into the distal tuft, which also then exhibits a Ca^{2+} transient (but see Xu et al. 2012).

NMDA spikes evoked focally by glutamate iontophoresis or 1-photon uncaging are associated with a local high calcium zone within ~10 μm of the input site, mirroring the distribution of activated NMDA channels (Major et al. 2008). This is accompanied by a lower (but above resting) calcium zone all the way to the dendritic tip, resulting most likely from calcium channels opening as the entire dendrite distal to the input site is depolarized: It is difficult for charge to escape from this segment. Simulations suggest that ~20% of the charge flow during an NMDA spike is via calcium conductances. The peak calcium in both zones increases with the spike/plateau duration (Major et al. 2008). Preliminary data suggest that brief NMDA spikes that result from distributed stimulation have correspondingly smaller, spread-out calcium transients, lacking a single obvious "hot zone" (Lavzin et al. 2012).

A key point is that at many dendritic locations it takes only a small number of synaptic inputs to evoke an NMDA spike: As few as ~10 clustered single spine inputs may suffice (**Figure 2**). This is a small fraction of the synapses on a single thin dendrite, typically

100–400 dendritic spines, depending on the species (Chen et al. 2011, Larkman et al. 1992). An equally crucial point is that NMDA spikes can also be elicited by distributed inputs (**Figure 2**): Clustering is not a prerequisite for a clear threshold. A third important point is that both depolarization and glutamate prebinding from previous activation reduce the glutamate threshold, allowing cooperativity between NMDA spikes [**Figure 2a,e**; **Supplemental Figure 1** (follow the **Supplemental Material link** from the Annual Reviews home page at **http://www.annualreviews.org**)] (Major et al. 2008, Polsky et al. 2009).

BIOPHYSICAL MECHANISMS OF NMDA SPIKES

A detailed discussion of the biophysical mechanisms of NMDA spikes is warranted because of their importance and prevalence in thin dendrites, which, as mentioned, receive the vast majority of inputs to pyramidal neurons.

NMDAR Channels

The properties of NMDAR channels have been reviewed extensively elsewhere (Paoletti 2011, Yuan et al. 2008). Here, we highlight important aspects relating to their regenerative nature. NMDARs are strongly electrogenic. Why would this characteristic have evolved if the sole function of NMDARs was synaptic plasticity? If their role was purely to detect and signal presynaptic-postsynaptic firing coincidences, using calcium influx to initiate a plasticity cascade, NMDARs could have been much smaller pure calcium conductances. As it is, however, typically ∼90% of the charge through NMDAR channels is actually carried by Na^+ and K^+ ions (Garaschuk et al. 1996, Jahr & Stevens 1993, Schneggenburger et al. 1993). Why? The calcium permeability of NMDAR channels can also be reduced drastically by activation of metabotropic γ-aminobutyric acid B ($GABA_B$) receptors (Chalifoux & Carter 2010) and by other kinds of plasticity (Sobczyk & Svoboda 2007), without appreciably altering the total current flow.
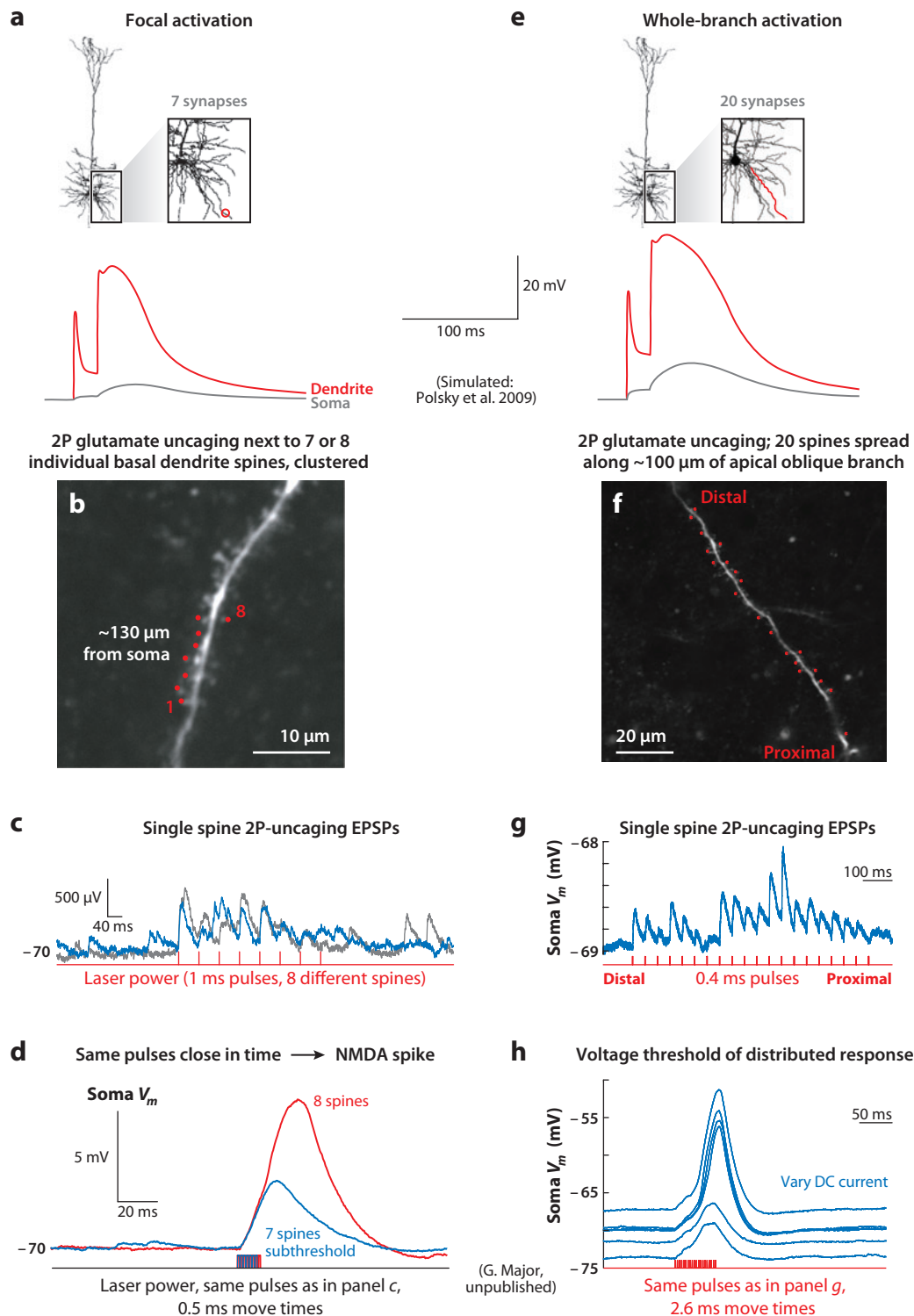
I-V Curve Families for a Unified Understanding of NMDAR Regenerative Events: Graded versus Thresholded

A helpful approach for understanding dendritic integration and spiking is to generalize the well-known idea of current-voltage relations (I-V curves). NMDA-dependent dendritic electrogenesis has both thresholded and graded aspects, both of which can be predicted from the basic I-V curve of the NMDAR conductance and can be unified under the same conceptual framework. From this perspective, the fundamental question for any given dendritic compartment is whether its instantaneous net I-V curve is N-shaped with three zero-current crossings (**Figure 3a**). If so, the membrane is bistable and is capable of firing a spike (of some kind) if kicked over the threshold. Following a pulse of glutamate onto a single electrical compartment of a dendrite, as the openable NMDAR conductance (g_{max}) rises, peaks, then falls, the instantaneous I-V relation progresses through a succession of different curves: an I-V movie (**Figure 3b**) (**Supplemental Videos 1–4**). The I-V curve starts downstable (blue). The right-hand trough progressively deepens, enhancing the N-shape. Eventually, if there is sufficient NMDA conductance, and other parameters allow, the I-V curve can morph into the bistable regime (green). If the voltage is then driven (or is already) above threshold, the membrane goes into the up state, and a spike/plateau results. This switches off by itself once the NMDA conductance falls back down below the minimum required for the I-V trough to dip below the zero-current axis, and the up state ceases to exist (**Figure 3b**: uppermost green curve → lowest blue curve; see below). A dendritic I-V relation is complex because it generally evolves over time. This is due in large part to synaptic conductances, which are major contributors and themselves rise and fall over time.

A spike is only all-or-none in the sense that it has some threshold below which it fails and above which it runs to completion.

a Focal activation

7 synapses

20 mV

100 ms

(Simulated:
Polsky et al. 2009)

Dendrite
Soma

e Whole-branch activation

20 synapses

b 2P glutamate uncaging next to 7 or 8
individual basal dendrite spines, clustered

~130 μm
from soma

8

1

10 μm

f 2P glutamate uncaging; 20 spines spread
along ~100 μm of apical oblique branch

Distal

Proximal

20 μm

c Single spine 2P-uncaging EPSPs

500 μV
40 ms

−70

Laser power (1 ms pulses, 8 different spines)

g Single spine 2P-uncaging EPSPs

−68

−69

Soma V_m (mV)

100 ms

Distal   0.4 ms pulses   Proximal

d Same pulses close in time ⟶ NMDA spike

Soma V_m

5 mV

20 ms

−70

8 spines

7 spines
subthreshold

Laser power, same pulses as in panel c,
0.5 ms move times

h Voltage threshold of distributed response

−55

−65

−75

Soma V_m (mV)

50 ms

Vary DC current

(G. Major,
unpublished)

Same pulses as in panel g,
2.6 ms move times

Figure 2

NMDA spikes can be elicited by stimulating a relatively small number of clustered or distributed synapses. (*a*, *e*) Neuron simulations; due to NMDAR priming, the second pulse of a paired-pulse stimulus produces an NMDA spike. *Other panels*: brain slice 2-photon glutamate uncaging experiments (layer 5). (*b*, *f*) Positions of uncaging spots (*red*) next to dendritic spines. (*c*, *g*) Corresponding single-spot uncaging EPSPs; similar to single synapse quantal EPSPs. (*d*, *h*) The same stimuli in quicker succession produce either a subthreshold response or an NMDA spike. (*d*) Blue traces = first 7 spots, red = all 8 spots stimulated, demonstrating glutamate threshold. (*h*) NMDA spike fails below a distinct voltage threshold.

All-or-none implies nothing about the constancy of that threshold, the stereotypy of the ensuing suprathreshold response, or the size or shape of that response relative to the biggest just-subthreshold response. This is, of course, not to mention further confusion caused by waveform changes as potentials propagate along a dendritic tree.

In large layer 5 pyramidal neuron basal dendrites, the NMDA spike glutamate threshold increases ∼5-fold from distal to proximal input sites, and the amplitude (reaching the soma) increases ∼7-fold (as does the maximal just-subthreshold response). These spatial gradients mirror the local input conductance (Major et al. 2008). If the stimulus is focal, once the response is suprathreshold, further increases in the stimulus produce relatively minor increases in the amplitude of the spike/plateau; however, the duration of the spike/plateau grows almost linearly with the stimulus and may reach hundreds of milliseconds (Major et al. 2008, Milojkovic et al. 2005a). This may serve as a prolonged time window for integration.

Investigators have shown experimentally that both features of NMDA regenerativity (graded and spike/plateau) exist, often simultaneously (Branco & Häusser 2011, Major et al. 2008, Schiller et al. 2000). Sharp thresholds for NMDA spikes have been found using focal synaptic stimulation (Gordon et al. 2006, Larkum et al. 2009, Nevian et al. 2007, Polsky et al. 2004, Schiller et al. 2000), glutamate UV-laser uncaging (Gordon et al. 2006, Major et al. 2008, Polsky et al. 2004, Schiller et al. 2000), and multispot two-photon uncaging (G. Major, unpublished observations; **Figure 2***b–d*). In addition, it seems plausible, a priori, that whereas focal stimulation can
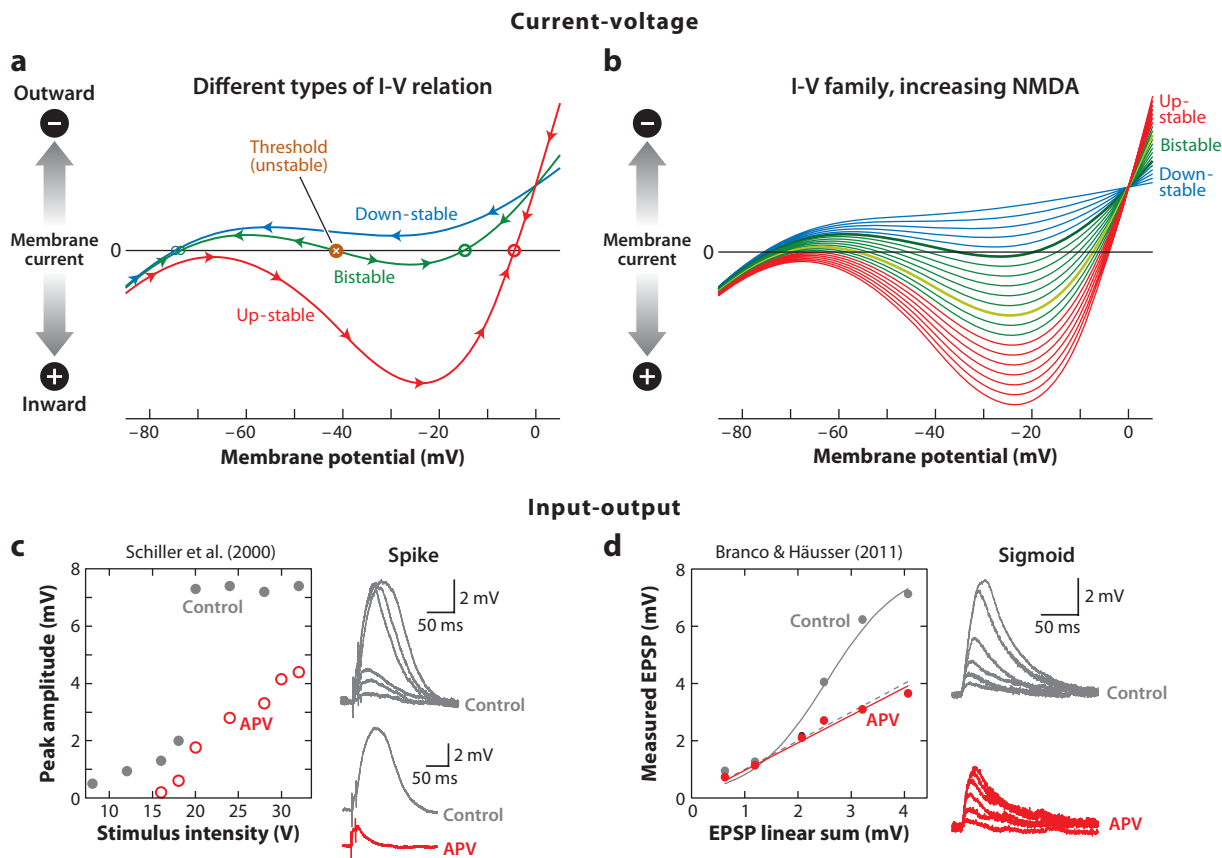
lead to sharp thresholds, highly distributed stimulation might be expected to lead to a blurring of thresholds and more sigmoidal input-output relations. In fact, perhaps counterintuitively, both experimental data and models show that distributed stimulation is still perfectly compatible with sharp thresholds (**Figure 2***e–h*; **Supplemental Figure 3***f–g*, discussed below).

Different experimental setups have found a range of NMDA regenerative behavior, from graded boosting to full-blown spikes. This range may reflect various laboratories exploring different regions within the space of possible dendritic NMDAR-dependent I-V curves (e.g., **Figure 3***b*). Experimental differences may be responsible, including, for example, the degree of input clustering/synchrony and effective AMPA/NMDA ratios. Covert spikes may also play a role (see below).

Partially Overlapping Time Courses of AMPAR and NMDAR Channels

Dendrites contain electrical mechanisms that operate over a range of time scales. At the fast end of the spectrum are AMPA receptor conductances, with decay time constants as short as ∼0.5 ms (or faster) at body temperature (Gardner et al. 2001, Postlethwaite et al. 2007, Zhang & Trussell 1994). These conductances are similar in time scale to those underlying the partially active backpropagation of APs, duration also ∼0.5 ms (Stuart et al. 1997), the fast voltage switching of NMDAR conductances [dominant time constants submillisecond (Kampa et al. 2004, Spruston et al. 1995a)], and the fast inward rectifier conductance (Yamada et al. 1998).

Current-voltage

a Different types of I-V relation

b I-V family, increasing NMDA

Input-output

c

d

Figure 3

Understanding threshold and spike size: instantaneous current-voltage (I-V) relations and bistability. (*a*) Three types of instantaneous I-V relation. Arrows indicate system flow; open circles indicate stable states. Details in **Supplemental Figure 4** (follow the **Supplemental Material link** from the Annual Reviews home page at **http://www.annualreviews.org**). (*b*) I-V curve shape changes smoothly as maximum openable NMDAR conductance increases, but curve type switches suddenly from downstable to bistable at a critical level of NMDAR conductance (and again from bistable to upstable if NMDA conductance rises enough). *Thick dark green*: just bistable I-V curve with a high threshold, and a small jump from threshold to upstate (**Supplemental Figure 4*c***). A large enough AMPA (2-amino-3-(3-hydroxy-5-methyl-isoxazol-4-yl)propanoic acid) component could kick the dendrite over the threshold, resulting in a small spike riding on a large PSP and a sigmoid input-output relation (I-O). *Thick light green:* bistable I-V curve with more NMDA conductance, a low threshold, and a big jump (**Supplemental Figure 4*e***). An input with a low AMPA fraction may reach this threshold, yielding a big spike on a small PSP, and a step-like I-O. See **Supplemental Videos 1–4**. (*c–d*) Experiments: somatic voltage transients from basal dendritic stimulation. (*c*) NMDA spike, step-like I-O. (*d*) More graded response, sigmoidal I-O. In both cases, nonlinearity was abolished by NMDAR block.

Supplemental Material

Substantially slower is the activation time course of the NMDAR upon binding glutamate: on the order of a few milliseconds (D'Angelo et al. 1994, Dalby & Mody 2003, Dzubay & Jahr 1996, Korinek et al. 2010, Popescu et al. 2004, Spruston et al. 1995a). An absolutely key point is that following a brief synaptic pulse of glutamate, from a

single presynaptic release event, most of the AMPAR conductance has died away before the NMDAR conductance is half primed or activatable, that is, capable of conducting, if depolarized (Stern et al. 1992). NMDARs must bind glutamate (and D-serine) and undergo internal conformational/state changes to become capable of magnesium unblock and

conducting (Kampa et al. 2004, Popescu et al. 2004), and these state changes take longer than their counterparts in AMPARs. The NMDAR decay time constant is even longer, probably ~40–60 ms. The range may be as broad as 10 to ~100 ms at body temperature, even if one restricts discussion to the faster NR2A subtype of the receptor more prevalent in adults. There is much uncertainty about Q_{10} values, which could be in the range of 1.7 to 2.4 (Dalby & Mody 2003, Korinek et al. 2010).

The observation that the AMPA current has largely decayed by the time the NMDA conductance has half primed is absolutely crucial to understanding what dendrites might be able to do and how they might do it: specifically whether they exhibit thresholds (details in next section). Note that when one considers NMDA spikes and plateaus, which are relatively slow events (half-width or duration at half amplitude ranges from ~20 ms to several hundred milliseconds or longer), the dendrites behave in a more electrically compact fashion than they would, say, for a backpropagating AP with a half-width of only 0.5 ms.

Sharpness of Threshold and Spike-Sigmoid Duality

Experiments (**Figure 3c,d**) and simulations suggest that thin dendrites can produce both sigmoid and step-like input-output (I-O) relations, depending on the input parameters. In full compartmental model simulations, sigmoidal I-O relations result from higher AMPA/NMDA ratios, slower AMPAR decay kinetics, more synchronous inputs, and more spatial spread of the inputs (**Supplemental Figures 2** and **3**). Conversely, lower AMPA/NMDA ratios, faster AMPAR decay, and more temporal but less spatial dispersion of inputs all conspire to produce more step-like I-O relations.

The simplest way to understand this process is from I-V curve movies. A large AMPA component produces a large voltage kick, which can cross the threshold at a relatively low NMDA conductance g_{max} (openable conductance), i.e.,

when the I-V curve is only just bistable and is still downskewed with a high barrier (downstate → threshold) and a small jump (threshold → upstate; **Figure 3b**, **Supplemental Figure 4c**). As a result, we see a small spike riding on a large subthreshold response (**Supplemental Videos 1** and **2**). If the input is increased further, the maximum response (upstate) grows in a graded manner. The net result is a sigmoidal I-O.

Conversely, a small AMPA component produces a small voltage kick; therefore, with a low AMPA/NMDA ratio, the NMDAR g_{max} can increase to a value at which the I-V curve is upskewed bistable before the AMPA kick is enough to cross the threshold (low barrier, big jump; **Figure 3b**, **Supplemental Figure 4e**). When it does cross the threshold, there is a big jump in response amplitude: a large spike riding on a small subthreshold response. The I-O relation is dominated by a sharp step. This is also true for intermediate cases in which the threshold is crossed when the I-V curve is symmetrically bistable (**Figure 3a**, **Supplemental Figure 4d**, **Supplemental Videos 3** and **4**).

Similar logic applies to the other input parameters. Slowing down the AMPAR decay allows the threshold to be crossed at a lower NMDAR conductance, producing a smaller spike riding on a bigger subthreshold response (**Figure 3**, **Supplemental Figures 2** and **4**). Desynchronizing the inputs is roughly equivalent to reducing the AMPA component: Time jitter has far less effect on the much slower NMDA component.

There is a further plot twist. Simulations suggest that essentially the same spike waveform can participate in both sigmoidal and stepped I-O relations (compare thick with thick, medium with medium, and dashed with dashed waveforms across panels in **Supplemental Figures 2** and **3**: Each of these is just above a clear glutamate threshold in at least one plot but is hidden within a sigmoid in at least one other plot). Thus, there is a degree of spike-sigmoid duality.

It is important that even spatially distributed inputs can produce stepped input-output relations with clear thresholds over a wide range

of biologically plausible parameters (**Figure 2**, **Supplemental Figure 3**). What actually happens in real life must now be settled with experiments in awake, behaving animals: The necessary technology is gradually becoming available.

Cooperativity

Depolarization reduces the NMDA spike glutamate threshold (Major et al. 2008, Polsky et al. 2009); this depolarization can be provided by another NMDA spike/plateau, including at a more distal location in the same dendrite (**Supplemental Figure 1**), leading to a number of interesting computational capabilities such as directionally biased responses, proximal-distal synapse interplay, and classical receptive field–contextual interactions (Behabadi et al. 2012, Branco et al. 2010, Major et al. 2008). Depolarizing drive (i.e., positive current), from whatever source, shifts the I-V curve vertically downward, which makes the bistable regime start at a lower glutamate-bound NMDAR conductance g_{max} (just a small shift converts the lower blue curve in **Figure 3b** to bistable). Within the bistable regime, this downward shift in the I-V curve has three effects at a given NMDAR g_{max}: The downstate moves more positive, the threshold more negative, and the upstate more positive (**Supplemental Figure 5**). This lowers the barrier to threshold but increases the jump above threshold [and the net spike amplitude (**Supplemental Figures 4** and **5**)], allowing the threshold to be crossed by a smaller AMPAR conductance; for a given AMPA/NMDA ratio, the I-O relation is shifted to the left (lower glutamate threshold) and becomes more stepped, with a bigger spike riding on a smaller PSP.

Inward Rectification

Bistability of instantaneous I-V curves can be made more robust (extended over a wider range of parameters) by several other conductances also conveniently found in dendrites, such as GABA$_A$ and fast inward rectifier potassium (KIR) channels (Sanders et al. 2013).

All neocortical pyramidal neurons investigated to date exhibit substantial inward rectification (their input resistance and time constants can decrease up to ~4-fold as the membrane potential is varied from around −50 mV to −90 mV (Major 1992, p. 72; Waters & Helmchen 2006). KIR channels are major players and are, in many ways, mirror images of NMDAR channels (Kashiwagi et al. 2002, Yamada et al. 1998). They have similar structures but are inverted in the membrane. KIR channels are blocked by intracellular (as opposed to extracellular) Mg^{2+}; they open rapidly with hyperpolarization: the opposite polarity to NMDARs. The symmetry between NMDA and KIR goes further still: Some types of KIR channel are even gated by transmitters, albeit more slowly via GABA$_B$ metabotropic receptors and G proteins (Yamada et al. 1998).

The left-hand part of an N-shaped I-V curve is selectively enhanced by adding inward rectifier conductance, which makes the overall N more symmetrical, strengthening the stability of the otherwise fragile downstate by providing more corrective current on either side (Sanders et al. 2013). This in turn expands the range of baseline voltages (DC current offsets) and inputs (e.g., NMDA conductances) compatible with instantaneous bistability and, more exactingly, a sharp dendritic spike threshold. Compared with a non-voltage-dependent K^+ conductance, by closing with depolarization, inward rectifier conductance moves the unstable threshold point to the left to more hyperpolarized voltages, while moving the upstate to the right. These shifts lower the barrier to threshold and increase the jump above threshold, leading to a more pronounced step in the I-O relation. Inward rectification could thus both increase the robustness and sharpen the threshold of dendritic spikes.

Inhibition

GABA$_A$ inhibition can similarly increase the robustness and extent (in parameter space) of the bistable regime, stabilizing the downstate not only by moving the I-V curve vertically

upward, but also by steepening it (Lisman et al. 1998). The price is a higher threshold (and an increase in the number of synapses required for an NMDA spike).

If negative current is injected within the same dendritic compartment, the I-V curve family shifts vertically upward (Jadi et al. 2012) (**Supplemental Figure 5**). For some parameter combinations this can destroy the bistability of weakly bistable curves, pushing the trough above the zero-current axis and rendering them downstable (**Figure 3**). In the case of more deeply bistable curves, negative current moves the threshold to the right and both down- and upstates to the left, raising the barrier but reducing the jump. If we start with a glutamate stimulus that elicits an NMDA spike and progressively hyperpolarize the cell, eventually a baseline voltage will be reached (prevention threshold), below which the same glutamate stimulus cannot push the dendrite across the threshold; thus the NMDA spike fails (**Figure 2b**) (Jadi et al. 2012, Major et al. 2008). If, however, an N-shaped I-V curve is initially upstable (**Figure 3a,b**) (e.g., relatively small leak/inward rectifier + large NMDA conductance), sufficient negative current can make it bistable by pushing the left-hand peak above the zero current axis.

Spike/Plateau Termination and Calcium-Activated Potassium Channels

However it gets there, once the dendrite is in an upstate, eventually the NMDA component starts to decay, and the level of the upstate (plateau top) declines slowly (this can be seen in experimental NMDA spike/plateau waveforms lasting more than ~40 ms, i.e., a couple of membrane time constants). After a time delay that may be several NMDAR decay time constants long, depending on the original safety factor,[2] the NMDA conductance falls

to the point where the right-hand local minimum of the N-shaped I-V curve slips just above the zero-current axis, and the upstate suddenly ceases to exist. A relatively rapid downstroke ensues, and the membrane ends up back in the downstate (now the only stable state). This decay of the plateau top (upstate) can be accelerated by calcium accumulation opening $gK_{Ca}s$, in particular the apamin-sensitive SK (small conductance) channel, which colocalizes with NMDARs in spines (Cai et al. 2004, Ngo-Anh et al. 2005, Wei et al. 2001). On the other hand, in other brain areas, calcium-activated nonspecific cation conductances can be activated, causing the reverse effect and leading to a much longer plateau (reviewed in Major & Tank 2004). At any time during the slow decline of the upstate, providing the I-V curve is bistable (not upstable), a sufficiently strong brief hyperpolarizing pulse, for example a GABA IPSP (inhibitory postsynaptic potential), could flip the dendrite prematurely into the downstate and curtail the NMDA spike/plateau.

CONCEPTUAL FRAMEWORK FOR UNDERSTANDING THE PYRAMIDAL NEURON: COMPARTMENTS, COMPUTATIONAL UNITS, CANONICAL DESCRIPTIONS
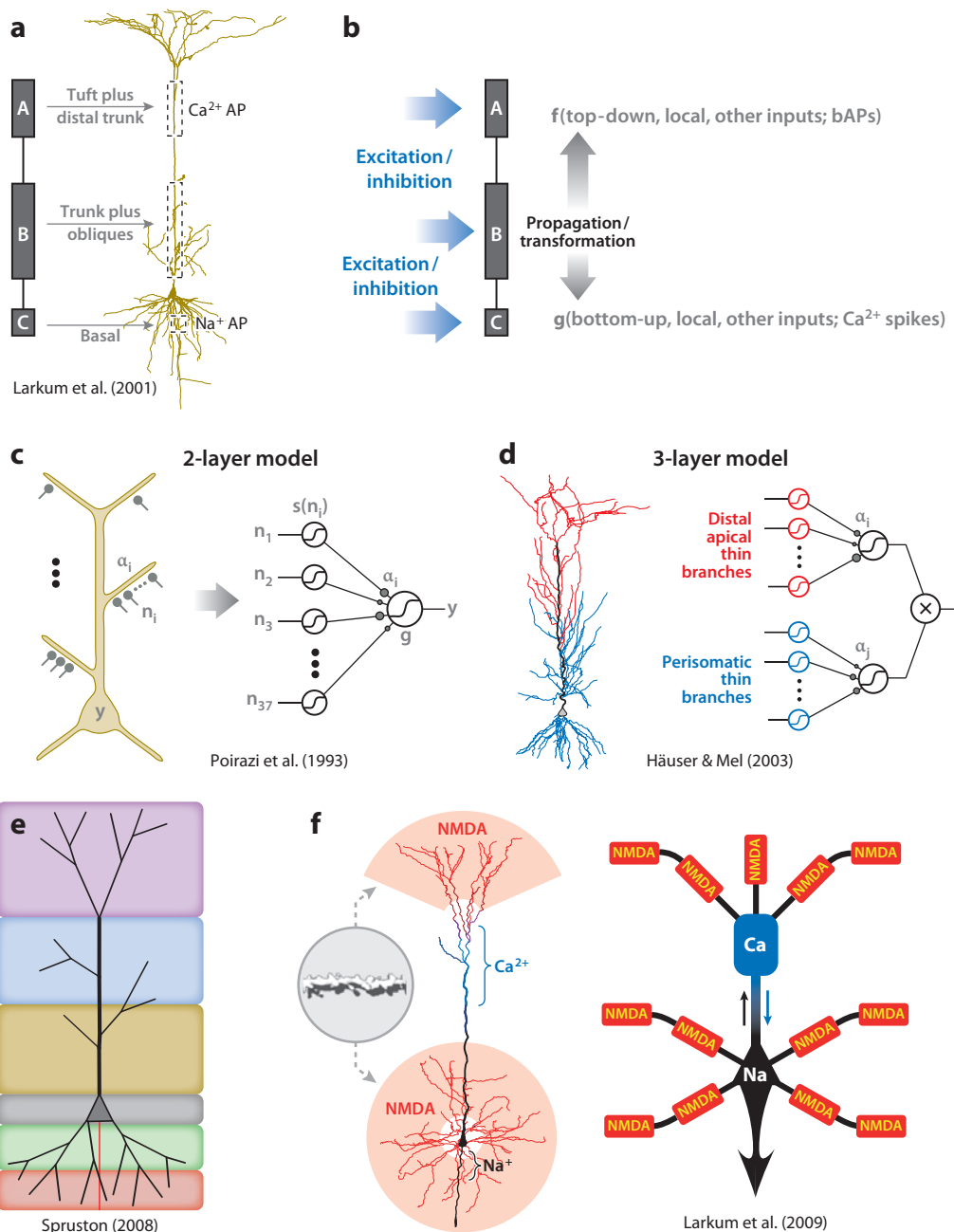
Canonical Abstractions

Taken together, the observations outlined above provide powerful constraints on models of neocortical pyramidal neurons. Actually understanding any given neuron requires the right level of abstraction (Branco & Häusser 2010, Häusser & Mel 2003, Herz et al. 2006, Koch et al. 1983, Koch & Segev 2000, Larkum et al. 2001, Mel 1994, Poirazi et al. 2003, Spruston 2008). The goal is to encapsulate the salient input/output properties of the neuron within a minimal description (Mirsky et al. 1998, Spruston 2008). Investigators have suggested several canonical abstractions for pyramidal cells (e.g., **Figure 4**).

---

[2]How many times more NMDA g_{max} (openable conductance) is present, at its peak, than required for bistability.

In the three-compartment (three-computational subunit) model (**Figure 4a,b**), the pyramidal neuron bauplan is split into three major dendritic arbors: basals, apical trunk/obliques, and distal trunk/tuft (Larkum et al. 2001); dendrites within each arbor are lumped together into a single functional compartment. This model also takes into account the location of the two major spike initiation zones, the axo-somatic sodium initiation zone and the distal apical calcium initiation zone, separated by the apical trunk (Amitai et al. 1993,

a

Tuft plus distal trunk — Ca²⁺ AP

Trunk plus obliques

Basal — Na⁺ AP

Larkum et al. (2001)

b

Excitation/inhibition

Excitation/inhibition

A — **f**(top-down, local, other inputs; bAPs)

Propagation/transformation

C — **g**(bottom-up, local, other inputs; Ca²⁺ spikes)

c 2-layer model

$s(n_i)$

n_1
n_2
n_3
α_i
g
y
n_{37}

Poirazi et al. (1993)

d 3-layer model

Distal apical thin branches — α_i

Perisomatic thin branches — α_j

$\times$

Häuser & Mel (2003)

e

Spruston (2008)

f

NMDA

Ca²⁺

NMDA

Na⁺

NMDA Ca NMDA Na

Larkum et al. (2009)

Figure 4

Encapsulating the properties of pyramidal neurons. (*a*, *b*) Three-compartment model of a layer 5 pyramidal neuron designed to include the influence of the three major dendritic arborizations: tuft + distal trunk (A), apical trunk/obliques (B), and basal dendrites (C). Each functional compartment incorporates/abstracts distinct electrical properties/channel distributions. Compartments A and C can initiate Ca^{2+} and Na^+ spikes, respectively; f(...) and g(...) represent their input-output functions. Excitatory and inhibitory influences act together on individual compartments. The tuft integrates prominent long-range top-down feedback with local and other inputs, but the threshold for generating output is modulated by backpropagating action potentials (bAPs, i.e., output spikes of the cell). The basal compartment integrates bottom-up, local, and other inputs but is influenced heavily by Ca^{2+} spikes in the tuft. The trunk modulates the coupling between the other two compartments. (*c*) 2-layer neuron; each dendrite behaves as a neural network neuron-like unit, sending weighted output to the soma. (*d*) 3-layer neuron; similar, but two major spike initiation zones integrate input from different subtrees and interact nonlinearly. (*e*) Compartmentalization based on cortical layer. Synaptic inputs from different sources arrive on dendrites in different layers, which may lead to functional domains within the dendritic tree. (*f*) Electrogenesis based on dendrite thickness. Most synaptic inputs are onto thin dendrites, dynamically changing segments or regions of which may produce local NMDA spikes; these interact bidirectionally with one another and with other inputs to influence the nearest of the two intrinsic conductance-based spike initiation zones, which also interact via bidirectional signals along the thick apical trunk (as in the three-compartment model).

Schiller et al. 1997, Yuste et al. 1994). Distal Ca^{2+} spikes greatly enhance the influence of the tuft; inputs that may otherwise have had a negligible effect on output firing can even come to dominate it: In large layer 5 pyramidal neurons, the Ca^{2+} spike generally contributes to a burst of somatic APs (Larkum & Zhu 2002, Williams & Stuart 1999, Zhu 2000). Basals and proximal obliques can be further collapsed together functionally, depending on the layer specificity of inputs (Briggs & Callaway 2005, Lübke & Feldmeyer 2007, Petreanu et al. 2009, Schubert et al. 2001). However, the apical trunk clearly has a special layer-spanning role that signals the output of each dendritic compartment to the others (Larkum et al. 1999, Larkum 2013).

The formalization of the cell in three compartments ignores the possibility of local computations performed in thin basal, oblique, and tuft dendrites, for instance with local NMDA and sodium spikes (Larkum et al. 2009, Losonczy & Magee 2006, Mel 1993, Polsky et al. 2004, Schiller et al. 2000). These local computations are partially captured by 2- and 3-layered feedforward network models (**Figure 4c,d**) (Häusser & Mel 2003, Mel 1993, Poirazi et al. 2003). Within this framework, local inputs are summed nonlinearly (e.g., sigmoidally) within fine dendritic branches and then integrated again at one or more main intrinsic spike initiation zones. However, these abstractions allow only unidirectional signaling, ignoring backpropagating APs and

cross talk or cooperativity between different dendrites or segments of dendrites (Major et al. 2008) (**Supplemental Figure 1**). Bidirectional signaling allows more complex processing capabilities (Behabadi et al. 2012, Branco et al. 2010, London et al. 2008). For instance, a ~30-ms time window exists for the detection of coincident tuft and basal inputs (Larkum et al. 1999, Polsky et al. 2004), which can be modified by the location/activity of the apical oblique dendrites (Schaefer et al. 2003).

Pyramidal neurons are embedded in a layered structure (the cortex); the distribution of synaptic input is constrained, e.g., tuft dendrites are likely to receive long-range inputs (Binzegger et al. 2004). Inputs from different sources are not randomly distributed but tend to terminate in a layer-specific manner (Briggs & Callaway 2005, Lübke & Feldmeyer 2007, Petreanu et al. 2009, Schubert et al. 2001). Such targeting may result in different functional compartmentalization in different neurons (**Figure 4e**). In the logical extreme, each individual thin dendrite could function as a multicompartmental unit with local NMDA-dependent computations (**Figure 4f**). This abstraction is, in effect, an extension of the three-compartment model, with dynamic bunches of extra NMDAR-dependent compartments, depending on the input pattern. Each functional compartment can be understood in terms of the I-V analysis presented above; interactions between compartments

can be understood via multidimensional I-V analysis (see **Supplemental Discussion**).

Functional Compartmentalization of Inputs in Thin Dendrites

Inclusion of the distribution of synaptic input as a key parameter complicates the issue of determining the most appropriate dendritic computational subunit (Häusser & Mel 2003, Polsky et al. 2004). The extent of functional compartmentalization becomes strongly dependent on the uniformity versus nonuniformity of both the intrinsic conductances and the pattern of inputs (extrinsic conductances). Leaving aside spatiotemporal sequences (Branco & Häusser 2011), one can start by differentiating between the case of fairly uniform versus clustered inputs (Larkum & Nevian 2008, Mel 1993). In the case of uniform input activation, it may be helpful to treat a terminal dendritic branch as a single computational unit (Poirazi et al. 2003). One can also lump several similar dendrites within a subtree into a single equivalent dendrite if they all receive comparable inputs. With very sparse activation, integration takes place in the linear/sublinear regime of input summation (see above). However, because of cooperativity between thin dendrites, we predict that increasing the density of activated inputs (<5%, see below) should be sufficient to initiate distributed regenerative boosting (Branco & Häusser 2011) or a distributed spike spread out over that group of branches (Lavzin et al. 2012).

In contrast with a random distribution of synapses, one of the leading hypotheses is that small clusters of synapses onto dendritic branchlets perform nonlinear local integration (Häusser & Mel 2003, Poirazi et al. 2003). In this framework, dendrites perform local computations such as calculating binocular rivalry (Archie & Mel 2000) and the direction of movement (Borst & Egelhaaf 1992, Branco et al. 2010, Major et al. 2008). Both modeling and experiments suggest that dendritic subunits are not fixed. They are dynamic and can change in size and location according to the input pattern (Larkum et al. 2009, Major et al. 2008,

Polsky et al. 2004). Even if neocortical connectivity were totally random and firing were sparse, random inputs may still be surprisingly clustered. Thus, the arrival of ~10 inputs onto the same dendritic branch could occur reasonably often. In fact, a number of studies suggest that synaptic input is not entirely random, which would accentuate clustering (Kleindienst et al. 2011, Takahashi et al. 2012).

Finally, inhibition targeted to certain portions of the dendritic tree could play a role in compartmentalizing the neuron (Palmer et al. 2012). In vivo, GABA inhibition is an important player that would be expected to keep NMDA spikes in check (Gentet et al. 2012, Jadi et al. 2012, Liu 2004, Rhodes 2006). Neighboring branches could be decoupled by inhibitory conductances, either synaptic or intrinsic (e.g., potassium conductances; see above).

Minimum Number of Synapses Required to Initiate an NMDA Spike

How many synapses are needed to evoke an NMDA spike, and what is the spatial distribution of these synapses? The effective AMPA/NMDA ratio is crucial because it influences both the likelihood of a local NMDA spike and the sharpness of its threshold. Numerous studies have investigated AMPA/NMDA ratios at excitatory synapses in different neocortical areas, and the maximal (openable) conductances are generally comparable: If anything, there may be more available NMDAR conductance than AMPAR conductance (Myme et al. 2003, Nimchinsky et al. 2004). In addition, NMDARs have ~100-fold higher glutamate affinity than do AMPARs (Patneau & Mayer 1990, Trussell & Fischbach 1989) and are far less prone to desensitization (Korinek et al. 2010, Trussell & Fischbach 1989, Vyklicky et al. 1990). Any desynchronization between inputs will tend to favor NMDA over AMPA components (see below). Thus under many stimulus/activity patterns in vivo, NMDAR conductances may dominate AMPAR conductances, particularly if firing rates or ambient glutamate is high. Even moderate levels of

glutamate are likely to desensitize AMPARs and prebind NMDARs, priming the latter to behave as purely depolarization-activated channels.

Modeling and two-photon spine uncaging data suggest that NMDA spikes in distal dendrites can be evoked by as few as ∼10 clustered single spine inputs (**Figure 2a–d**) or by ∼20 inputs distributed randomly along much of the dendrite's length (**Figure 2e–h**) (Major et al. 2008, Polsky et al. 2009; G. Major, unpublished observations). Using the two-photon uncaging method, a wide range of uncaging EPSP sizes can be dialed up at a particular dendritic spine, from zero to several times larger than the typical miniature (single synapse?) EPSP, simply by varying the intensity or location of the uncaging laser pulses (and/or the concentration of caged glutamate). Uncertainty over the correct average miniature EPSP size (and the "correct" AMPA/NMDA ratio) therefore complicates the interpretation of the number of synapses needed. Nevertheless, a typical terminal dendritic branch bears hundreds of dendritic spines (Larkman 1991), which represents a massive safety margin: Only a small fraction of the total synapses onto a branch may need to be activated, maybe as few as 5%.

The threshold number is only a rough estimate and will change as a function of baseline membrane potential. Depolarization reduces the glutamate threshold, allowing cooperativity between NMDA spikes from different locations (see above). The threshold number of synapses will also change with the NMDA/AMPA ratio, depending on the recent history of glutamate and coagonist exposure. In addition, any conductances with broadly similar I-V relations to NMDARs, e.g., depolarization-activated Na^+ or Ca^{2+} channels, will reduce the amount of NMDA conductance required to achieve a certain sharpness of threshold (Major et al. 2008, Schiller et al. 2000)—an effect similar to boosting the NMDA/AMPA ratio.

NMDA SPIKES IN VIVO

Dendritic NMDA spikes were discovered in brain slices, and their fundamental properties have been extensively characterized in vitro. NMDA spikes are very robust in thin dendrites of excitatory neurons in all neocortical layers and areas so far tested, with a large safety factor (Branco & Häusser 2011, Gordon et al. 2006, Larkum et al. 2009, Lavzin et al. 2012, Major et al. 2008, Nevian et al. 2007, Schiller et al. 2000).[3]

In vivo, investigators may already have made tantalizing preliminary sightings of events involving NMDA spike/plateaus, supporting the participation of NMDAR regenerativity across the board, from receptive fields to working memory and beyond (Coyle et al. 2003, Daw et al. 1993, de Kock et al. 2007, Major & Tank 2004, Self et al. 2012). A recent in vivo whole-cell patch recording study found a substantial NMDAR component in the angular tuning and artificial whisking responses of layer-4 barrel cortex neurons, which was blocked by an intracellular NMDAR blocker (MK801) or by membrane hyperpolarization, both of which have minimal effects on the rest of the circuit (Lavzin et al. 2012). Modeling suggests that the most likely explanation for the size and duration of the NMDAR-dependent component is dendritic NMDAR-dependent regenerative responses, potentially including multi-branch/globally scattered NMDA spikes.

Large, distributed Ca^{2+} transients have been observed in the apical tufts of layer 5 neurons in the somatosensory cortex during sensorimotor behaviors involving active touch (Xu et al. 2012). A plausible explanation is that these Ca^{2+} transients are caused by distal plateau potentials, which are greatly enhanced by top-town excitatory inputs into the tuft. This is what would be expected for distributed tuft NMDA spike/plateaus triggering and cooperatively interacting with Ca^{2+} spike/plateaus in the distal apical trunk/proximal tuft Ca^{2+} zone. Equally intriguingly, voltage-dependent place fields have recently been observed in CA1 pyramidal cells, recorded whole-cell during active

---

[3]Diameter less than ∼1.5 μm, with the possible exception of thin apical trunks (and very proximal basal segments).

maze exploration (Lee et al. 2012). Depolarizing events underlying place field firing appear above a distinct (somatic) voltage threshold in each cell and vanish into noise at more hyperpolarized membrane potentials. Again, this is exactly what one might expect if an important role was played by NMDAR-dependent dendritic regenerative excitation, conditional on the network firing pattern.

Some studies appear to indicate that, at least under some conditions in vivo (e.g., visual gratings, anesthesia), summation of inputs can be essentially linear (Jagadeesh et al. 1993). Recent reports combining two-photon imaging with whole-cell recordings in vivo from layer 2/3 pyramidal neurons in mouse visual, somatosensory, and auditory cortices also noted a lack of participation of dendritic regenerative mechanisms (Chen et al. 2011, Jia et al. 2010, Varga et al. 2011). However, these experiments were performed in unfavorable conditions for dendritic spike generation, including using anesthetized animals and keeping the resting membrane potential below AP threshold, which generally requires negative current injection [for examples of NMDAR regenerativity being blocked by hyperpolarization, see Lavzin et al. (2012)]. Despite these experimental conditions, sensory stimulation evoked scattered dendritic calcium hot spots with transients similar in size to those from several backpropagating APs. Hot spots and spine transients were substantially reduced by NMDAR blockers (including intracellular MK801), pointing to a possible role for regenerative NMDAR activation. Moreover, the number of activated spines per dendrite in vivo (up to ∼30 per 100 μm) reported in these studies may well be in the appropriate range for triggering NMDA spikes, given that not all spines were visible (Chen et al.

2011, Varga et al. 2011). It is crucial to emphasize that an NMDA spike does not require neighboring spines to have the same receptive fields/stimulus preferences, nor does it require coactivation of neighboring spines (clustering), nor (if brief and distributed) will it necessarily produce large dendritic shaft Ca^{2+} transients [especially if the NMDAR Ca^{2+} permeability is reduced (Chalifoux & Carter 2010)]. The slow Ca^{2+} transients observed in vivo (Chen et al. 2011, Jia et al. 2010) are consistent with the time courses of NMDA spike/plateaus but appear far slower than what one might expect from single quantal synaptic events.

The functional consequences of NMDA spike/plateaus for cortical processing are potentially versatile and may depend on the cortical region. NMDA plateaus could help sustain network upstates and the persistent firing needed for working memory in the prefrontal cortex and other areas (Antic et al. 2010, Major & Tank 2004, Milojkovic et al. 2005a, Sanders et al. 2013). NMDA spikes could also create and sharpen receptive field selectivity in primary cortices and contribute to top-down/bottom-up interactions (Self et al. 2012), perhaps even within individual dendrites. Combined in vivo dendritic voltage and calcium recording is still in its infancy, but in the not-too-distant future, this method should begin to reveal whether regenerative events or spikes do indeed occur in thin dendrites (and if so, which type). Researchers have barely begun to explore the vast parameter space of possible brain states, neuronal types, dendritic recording sites, and stimuli: Dogma is premature, particularly in light of brain slice experiments suggesting that the biophysical machinery is present in abundance, with a massive safety factor, to support highly nonlinear input summation.

DISCLOSURE STATEMENT

LITERATURE CITED

Agmon-Snir H, Segev I. 1993. Signal delay and input synchronization in passive dendritic structures. *J. Neurophysiol.* 70:2066–85

Amitai Y, Friedman A, Connors BW, Gutnick MJ. 1993. Regenerative activity in apical dendrites of pyramidal cells in neocortex. *Cereb. Cortex* 3:26–38

Antic SD, Zhou WL, Moore AR, Short SM, Ikonomu KD. 2010. The decade of the dendritic NMDA spike. *J. Neurosci. Res.* 88:2991–3001

Archie KA, Mel BW. 2000. A model for intradendritic computation of binocular disparity. *Nat. Neurosci.* 3:54–63

Ariav G, Polsky A, Schiller J. 2003. Submillisecond precision of the input-output transformation function mediated by fast sodium dendritic spikes in basal dendrites of CA1 pyramidal neurons. *J. Neurosci.* 23:7750–58

Azouz R, Gray CM. 2000. Dynamic spike threshold reveals a mechanism for synaptic coincidence detection in cortical neurons in vivo. *Proc. Natl. Acad. Sci. USA* 97:8110–15

Behabadi BF, Polsky A, Jadi M, Schiller J, Mel BW. 2012. Location-dependent excitatory synaptic interactions in pyramidal neuron dendrites. *PLoS Comput. Biol.* 8(7):e1002599

Berger T, Larkum ME, Lüscher HR. 2001. High I(h) channel density in the distal apical dendrite of layer V pyramidal cells increases bidirectional attenuation of EPSPs. *J. Neurophysiol.* 85:855–68

Berger T, Lüscher HR. 2003. Timing and precision of spike initiation in layer V pyramidal cells of the rat somatosensory cortex. *Cereb. Cortex* 13:274–81

Binzegger T, Douglas RJ, Martin KA. 2004. A quantitative map of the circuit of cat primary visual cortex. *J. Neurosci.* 24:8441–53

Borst A, Egelhaaf M. 1992. In vivo imaging of calcium accumulation in fly interneurons as elicited by visual motion stimulation. *Proc. Natl. Acad. Sci. USA* 89:4139–43

Branco T, Clark BA, Häusser M. 2010. Dendritic discrimination of temporal input sequences in cortical neurons. *Science* 329:1671–75

Branco T, Häusser M. 2010. The single dendritic branch as a fundamental functional unit in the nervous system. *Curr. Opin. Neurobiol.* 20:494–502

Branco T, Häusser M. 2011. Synaptic integration gradients in single cortical pyramidal cell dendrites. *Neuron* 69:885–92

Briggs F, Callaway EM. 2005. Laminar patterns of local excitatory input to layer 5 neurons in macaque primary visual cortex. *Cereb. Cortex* 15:479–88

Byerly L, Masuda MO. 1979. Voltage-clamp analysis of the potassium current that produces a negative-going action potential in Ascaris muscle. *J. Physiol.* 288:263–84

Cai X, Liang CW, Muralidharan S, Kao JP, Tang CM, Thompson SM. 2004. Unique roles of SK and Kv4.2 potassium channels in dendritic integration. *Neuron* 44:351–64

Cash S, Yuste R. 1999. Linear summation of excitatory inputs by CA1 pyramidal neurons. *Neuron* 22:383–94

Cauller LJ, Connors BW. 1994. Synaptic physiology of horizontal afferents to layer-I in slices of rat SI neocortex. *J. Neurosci.* 14:751–62

Chalifoux JR, Carter AG. 2010. GABAB receptors modulate NMDA receptor calcium signals in dendritic spines. *Neuron* 66:101–13

Chen X, Leischner U, Rochefort NL, Nelken I, Konnerth A, et al. 2011. Functional mapping of single spines in cortical neurons in vivo. *Nature* 475:501–5

Coyle JT, Tsai G, Goff D. 2003. Converging evidence of NMDA receptor hypofunction in the pathophysiology of schizophrenia. *Ann. N. Y. Acad. Sci.* 1003:318–27

Dalby NO, Mody I. 2003. Activation of NMDA receptors in rat dentate gyrus granule cells by spontaneous and evoked transmitter release. *J. Neurophysiol.* 90:786–97

D'Angelo E, Rossi P, Taglietti V. 1994. Voltage-dependent kinetics of N-methyl-D-aspartate synaptic currents in rat cerebellar granule cells. *Eur. J. Neurosci.* 6:640–45

Dantzker JL, Callaway EM. 2000. Laminar sources of synaptic input to cortical inhibitory interneurons and pyramidal neurons. *Nat. Neurosci.* 3:701–7

Daw NW, Stein PS, Fox K. 1993. The role of NMDA receptors in information processing. *Annu. Rev. Neurosci.* 16:207–22

de Kock CP, Bruno RM, Spors H, Sakmann B. 2007. Layer- and cell-type-specific suprathreshold stimulus representation in rat primary somatosensory cortex. *J. Physiol.* 581:139–54

de Polavieja GG, Harsch A, Kleppe I, Robinson HP, Juusola M. 2005. Stimulus history reliably shapes action potential waveforms of cortical neurons. *J. Neurosci.* 25:5657–65

Dzubay JA, Jahr CE. 1996. Kinetics of NMDA channel opening. *J. Neurosci.* 16:4129–34

Garaschuk O, Schneggenburger R, Schirra C, Tempia F, Konnerth A. 1996. Fractional Ca^{2+} currents through somatic and dendritic glutamate receptor channels of rat hippocampal CA1 pyramidal neurones. *J. Physiol.* 491:757–72

Gardner SM, Trussell LO, Oertel D. 2001. Correlation of AMPA receptor subunit composition with synaptic input in the mammalian cochlear nuclei. *J. Neurosci.* 21:7428–37

Gentet LJ, Kremer Y, Taniguchi H, Huang ZJ, Staiger JF, Petersen CC. 2012. Unique functional properties of somatostatin-expressing GABAergic neurons in mouse barrel cortex. *Nat. Neurosci.* 15:607–12

Gordon U, Polsky A, Schiller J. 2006. Plasticity compartments in basal dendrites of neocortical pyramidal neurons. *J. Neurosci.* 26:12717–26

Gulledge AT, Kampa BM, Stuart GJ. 2005. Synaptic integration in dendritic trees. *J. Neurobiol.* 64:75–90

Hardingham NR, Read JC, Trevelyan AJ, Nelson JC, Jack JJ, Bannister NJ. 2010. Quantal analysis reveals a functional correlation between presynaptic and postsynaptic efficacy in excitatory connections from rat neocortex. *J. Neurosci.* 30:1441–51

Häusser M, Mel B. 2003. Dendrites: bug or feature? *Curr. Opin. Neurobiol.* 13:372–83

Häusser M, Spruston N, Stuart GJ. 2000. Diversity and dynamics of dendritic signaling. *Science* 290:739–44

Herz AV, Gollisch T, Machens CK, Jaeger D. 2006. Modeling single-neuron dynamics and computations: a balance of detail and abstraction. *Science* 314:80–85

Jadi M, Polsky A, Schiller J, Mel BW. 2012. Location-dependent effects of inhibition on local spiking in pyramidal neuron dendrites. *PLoS Comput. Biol.* 8:e1002550

Jagadeesh B, Wheat HS, Ferster D. 1993. Linearity of summation of synaptic potentials underlying direction selectivity in simple cells of the cat visual cortex. *Science* 262:1901–4

Jahr CE, Stevens CF. 1993. Calcium permeability of the N-methyl-D-aspartate receptor channel in hippocampal neurons in culture. *Proc. Natl. Acad. Sci. USA* 90:11573–77

Jia H, Rochefort NL, Chen X, Konnerth A. 2010. Dendritic organization of sensory input to cortical neurons in vivo. *Nature* 464:1307–12

Johnston D, Magee JC, Colbert CM, Cristie BR. 1996. Active properties of neuronal dendrites. *Annu. Rev. Neurosci.* 19:165–86

Judkewitz B, Roth A, Häusser M. 2006. Dendritic enlightenment: using patterned two-photon uncaging to reveal the secrets of the brain's smallest dendrites. *Neuron* 50:180–83

Kampa BM, Clements J, Jonas P, Stuart GJ. 2004. Kinetics of Mg^{2+} unblock of NMDA receptors: implications for spike-timing dependent synaptic plasticity. *J. Physiol.* 556:337–45

Kashiwagi K, Masuko T, Nguyen CD, Kuno T, Tanaka I, et al. 2002. Channel blockers acting at N-methyl-D-aspartate receptors: differential effects of mutations in the vestibule and ion channel pore. *Mol. Pharmacol.* 61:533–45

Kleindienst T, Winnubst J, Roth-Alpermann C, Bonhoeffer T, Lohmann C. 2011. Activity-dependent clustering of functional synaptic inputs on developing hippocampal dendrites. *Neuron* 72:1012–24

Koch C, Poggio T, Torre V. 1983. Nonlinear interactions in a dendritic tree: localization, timing, and role in information processing. *Proc. Natl. Acad. Sci. USA* 80:2799–802

Koch C, Segev I. 2000. The role of single neurons in information processing. *Nat. Neurosci.* 3(Suppl.):1171–77

Kole MH, Hallermann S, Stuart GJ. 2006. Single Ih channels in pyramidal neuron dendrites: properties, distribution, and impact on action potential output. *J. Neurosci.* 26:1677–87

Kole MH, Stuart GJ. 2008. Is action potential threshold lowest in the axon? *Nat. Neurosci.* 11:1253–55

Korinek M, Sedlacek M, Cais O, Dittert I, Vyklicky L Jr. 2010. Temperature dependence of N-methyl-D-aspartate receptor channels and N-methyl-D-aspartate receptor excitatory postsynaptic currents. *Neuroscience* 165:736–48

Larkman AU. 1991. Dendritic morphology of pyramidal neurones of the visual cortex of the rat: III. Spine distributions. *J. Comp. Neurol.* 306:332–43

Larkman AU, Major G, Stratford KJ, Jack JJ. 1992. Dendritic morphology of pyramidal neurones of the visual cortex of the rat. IV: Electrical geometry. *J. Comp. Neurol.* 323:137–52

Larkum M. 2013. A cellular mechanism for cortical associations: an organizing principle for the cerebral cortex. *Trends Neurosci.* 36:141–51

Larkum ME, Nevian T. 2008. Synaptic clustering by dendritic signalling mechanisms. *Curr. Opin. Neurobiol.* 18(3):321–31

Larkum ME, Nevian T, Sandler M, Polsky A, Schiller J. 2009. Synaptic integration in tuft dendrites of layer 5 pyramidal neurons: a new unifying principle. *Science* 325:756–60

Larkum ME, Zhu JJ. 2002. Signaling of layer 1 and whisker-evoked Ca^{2+} and Na^+ action potentials in distal and terminal dendrites of rat neocortical pyramidal neurons in vitro and in vivo. *J. Neurosci.* 22:6991–7005

Larkum ME, Zhu JJ, Sakmann B. 1999. A new cellular mechanism for coupling inputs arriving at different cortical layers. *Nature* 398:338–41

Larkum ME, Zhu JJ, Sakmann B. 2001. Dendritic mechanisms underlying the coupling of the dendritic with the axonal action potential initiation zone of adult rat layer 5 pyramidal neurons. *J. Physiol.* 533:447–66

Lavzin M, Rapoport S, Polsky A, Garion L, Schiller J. 2012. Non-linear dendritic processing determines angular tuning of barrel cortex neurons in-vivo. *Nature* 490:397–401

Lee D, Lin B-J, Lee AK. 2012. Hippocampal place fields emerge upon single-cell manipulation of excitability during behavior. *Science* 337:849–53

Lisman JE, Fellous JM, Wang XJ. 1998. A role for NMDA-receptor channels in working memory. *Nat. Neurosci.* 1:273–75

Liu G. 2004. Local structural balance and functional interaction of excitatory and inhibitory synapses in hippocampal dendrites. *Nat. Neurosci.* 7:373–79

Llinás R, Nicholson C, Freeman JA, Hillman DE. 1968. Dendritic spikes and their inhibition in alligator Purkinje cells. *Science* 160:1132–35

London M, Häusser M. 2005. Dendritic computation. *Annu. Rev. Neurosci.* 28:503–32

London M, Larkum ME, Hausser M. 2008. Predicting the synaptic information efficacy in cortical layer 5 pyramidal neurons using a minimal integrate-and-fire model. *Biol. Cybern.* 99:393–401

Losonczy A, Magee JC. 2006. Integrative properties of radial oblique dendrites in hippocampal CA1 pyramidal neurons. *Neuron* 50:291–307

Lübke J, Feldmeyer D. 2007. Excitatory signal flow and connectivity in a cortical column: focus on barrel cortex. *Brain Struct. Funct.* 212:3–17

Magee JC. 2000. Dendritic integration of excitatory synaptic input. *Nat. Rev. Neurosci.* 1:181–90

Major G. 1992. *The physiology, morphology and modelling of cortical pyramidal neurones.* PhD thesis. Oxford Univ., Oxford, UK

Major G, Larkman AU, Jonas P, Sakmann B, Jack JJ. 1994. Detailed passive cable models of whole-cell recorded CA3 pyramidal neurons in rat hippocampal slices. *J. Neurosci.* 14:4613–38

Major G, Polsky A, Denk W, Schiller J, Tank DW. 2008. Spatiotemporally graded NMDA spike/plateau potentials in basal dendrites of neocortical pyramidal neurons. *J. Neurophysiol.* 99:2584–601

Major G, Tank DW. 2004. Persistent neural activity: prevalence and mechanisms. *Curr. Opin. Neurobiol.* 14:675–84

McCormick DA, Shu Y, Yu Y. 2007. Neurophysiology: Hodgkin and Huxley model—still standing? *Nature* 445:E1–2; discussion E2–3

Mel BW. 1993. Synaptic integration in an excitable dendritic tree. *J. Neurophysiol.* 70:1086–101

Mel BW. 1994. Information processing in dendritic trees. *Neural Comput.* 6:1031–85

Migliore M, Shepherd GM. 2002. Emerging rules for the distributions of active dendritic conductances. *Nat. Rev. Neurosci.* 3:362–70

Milojkovic BA, Radojicic MS, Antic SD. 2005a. A strict correlation between dendritic and somatic plateau depolarizations in the rat prefrontal cortex pyramidal neurons. *J. Neurosci.* 25:3940–51

Milojkovic BA, Radojicic MS, Goldman-Rakic PS, Antic SD. 2004. Burst generation in rat pyramidal neurones by regenerative potentials elicited in a restricted part of the basilar dendritic tree. *J. Physiol.* 558:193–211

Milojkovic BA, Wuskell JP, Loew LM, Antic SD. 2005b. Initiation of sodium spikelets in basal dendrites of neocortical pyramidal neurons. *J. Membr. Biol.* 208:155–69

Milojkovic BA, Zhou WL, Antic SD. 2007. Voltage and calcium transients in basal dendrites of the rat prefrontal cortex. *J. Physiol.* 585(Pt. 2):447–68

Mirsky JS, Nadkarni PM, Healy MD, Miller PL, Shepherd GM. 1998. Database tools for integrating and searching membrane property data correlated with neuronal morphology. *J. Neurosci. Methods* 82:105–21

Myme CI, Sugino K, Turrigiano GG, Nelson SB. 2003. The NMDA-to-AMPA ratio at synapses onto layer 2/3 pyramidal neurons is conserved across prefrontal and visual cortices. *J. Neurophysiol.* 90:771–79

Nevian T, Larkum ME, Polsky A, Schiller J. 2007. Properties of basal dendrites of layer 5 pyramidal neurons: a direct patch-clamp recording study. *Nat. Neurosci.* 10:206–14

Ngo-Anh TJ, Bloodgood BL, Lin M, Sabatini BL, Maylie J, Adelman JP. 2005. SK channels and NMDA receptors form a Ca^{2+}-mediated feedback loop in dendritic spines. *Nat. Neurosci.* 8:642–49

Nimchinsky EA, Yasuda R, Oertner TG, Svoboda K. 2004. The number of glutamate receptors opened by synaptic stimulation in single hippocampal spines. *J. Neurosci.* 24:2054–64

Palmer LM, Schulz JM, Murphy SC, Ledergerber D, Murayama M, Larkum ME. 2012. The cellular basis of $GABA_B$-mediated interhemispheric inhibition. *Science* 335:989–93

Paoletti P. 2011. Molecular basis of NMDA receptor functional diversity. *Eur. J. Neurosci.* 33:1351–65

Patneau DK, Mayer ML. 1990. Structure-activity relationships for amino acid transmitter candidates acting at N-methyl-D-aspartate and quisqualate receptors. *J. Neurosci.* 10:2385–99

Petreanu L, Mao T, Sternson SM, Svoboda K. 2009. The subcellular organization of neocortical excitatory connections. *Nature* 457:1142–45

Platkiewicz J, Brette R. 2011. Impact of fast sodium channel inactivation on spike threshold dynamics and synaptic integration. *PLoS Comput. Biol.* 7:e1001129

Poirazi P, Brannon T, Mel BW. 2003. Pyramidal neuron as two-layer neural network. *Neuron* 37:989–99

Polsky A, Mel B, Schiller J. 2009. Encoding and decoding bursts by NMDA spikes in basal dendrites of layer 5 pyramidal neurons. *J. Neurosci.* 29:11891–903

Polsky A, Mel BW, Schiller J. 2004. Computational subunits in thin dendrites of pyramidal cells. *Nat. Neurosci.* 7:621–27

Popescu G, Robert A, Howe JR, Auerbach A. 2004. Reaction mechanism determines NMDA receptor response to repetitive stimulation. *Nature* 430:790–93

Postlethwaite M, Hennig MH, Steinert JR, Graham BP, Forsythe ID. 2007. Acceleration of AMPA receptor kinetics underlies temperature-dependent changes in synaptic strength at the rat calyx of Held. *J. Physiol.* 579:69–84

Priebe NJ, Ferster D. 2010. Neuroscience: each synapse to its own. *Nature* 464:1290–91

Rall W. 1964. Theoretical significance of dendritic trees for neuronal input-output relations. In *Neural Theory and Modeling*, ed. R Reiss, pp. 73–97. Stanford, CA: Stanford Univ. Press

Rall W. 1977. Core conductor theory and cable properties of neurons. In *Handbook of Physiology, the Nervous System, Cellular Biology of Neurons*. Sect. 1. Vol. 1, Part 1, ed. ER Kandel, pp. 39–98. Bethesda, MD: Am. Physiol. Soc.

Rapp M, Yarom Y, Segev I. 1996. Modeling back propagating action potential in weakly excitable dendrites of neocortical pyramidal cells. *Proc. Natl. Acad. Sci. USA* 93:11985–90

Rhodes P. 2006. The properties and implications of NMDA spikes in neocortical pyramidal cells. *J. Neurosci.* 26:6704–15

Rhodes PA. 1999. Functional implications of active currents in the dendrites of pyramidal neurons. In *Cerebral Cortex*, Vol. 13, ed. PS Ulinski, EG Jones, A Peters, pp. 139–200. New York: Plenum

Rhodes PA, Llinas RR. 2001. Apical tuft input efficacy in layer 5 pyramidal cells from rat visual cortex. *J. Physiol.* 536:167–87

Rinzel J, Rall W. 1974. Transient response in a dendritic neuron model for current injected at one branch. *Biophys. J.* 14:759–90

Sanders H, Berends M, Major G, Goldman MS, Lisman JE. 2013. NMDA and $GABA_B$ (KIR) conductances: the "perfect couple" for bistability. *J. Neurosci.* 33:424–29

Schaefer AT, Larkum ME, Sakmann B, Roth A. 2003. Coincidence detection in pyramidal neurons is tuned by their dendritic branching pattern. *J. Neurophysiol.* 89:3143–54

Schiller J, Major G, Koester HJ, Schiller Y. 2000. NMDA spikes in basal dendrites of cortical pyramidal neurons. *Nature* 404:285–89

Schiller J, Schiller Y. 2001. NMDA receptor-mediated dendritic spikes and coincident signal amplification. *Curr. Opin. Neurobiol.* 11:343–48

Schiller J, Schiller Y, Stuart G, Sakmann B. 1997. Calcium action potentials restricted to distal apical dendrites of rat neocortical pyramidal neurons. *J. Physiol.* 505(Pt. 3):605–16

Schneggenburger R, Zhou Z, Konnerth A, Neher E. 1993. Fractional contribution of calcium to the cation current through glutamate receptor channels. *Neuron* 11:133–43

Schubert D, Staiger JF, Cho N, Kotter R, Zilles K, Luhmann HJ. 2001. Layer-specific intracolumnar and transcolumnar functional connectivity of layer V pyramidal cells in rat barrel cortex. *J. Neurosci.* 21:3580–92

Schwindt P, Crill W. 1999. Mechanisms underlying burst and regular spiking evoked by dendritic depolarization in layer 5 cortical pyramidal neurons. *J. Neurophysiol.* 81:1341–54

Schwindt PC, Crill WE. 1997. Local and propagated dendritic action potentials evoked by glutamate iontophoresis on rat neocortical pyramidal neurons. *J. Neurophysiol.* 77:2466–83

Self MW, Kooijmans RN, Super H, Lamme VA, Roelfsema PR. 2012. Different glutamate receptors convey feedforward and recurrent processing in macaque V1. *Proc. Natl. Acad. Sci. USA* 109:11031–36

Shu Y, Hasenstaub A, Duque A, Yu Y, McCormick DA. 2006. Modulation of intracortical synaptic potentials by presynaptic somatic membrane potential. *Nature* 441:761–65

Sobczyk A, Svoboda K. 2007. Activity-dependent plasticity of the NMDA-receptor fractional Ca(2+) current. *Neuron* 53:17–24

Spruston N. 2008. Pyramidal neurons: dendritic structure and synaptic integration. *Nat. Rev. Neurosci.* 9:206–21

Spruston N, Jaffe DB, Johnston D. 1994. Dendritic attenuation of synaptic potentials and currents: the role of passive membrane properties. *Trends Neurosci.* 17:161–66

Spruston N, Jonas P, Sakmann B. 1995a. Dendritic glutamate receptor channels in rat hippocampal CA3 and CA1 pyramidal neurons. *J. Physiol.* 482(Pt. 2):325–52

Spruston N, Schiller Y, Stuart G, Sakmann B. 1995b. Activity-dependent action-potential invasion and calcium influx into hippocampal CA1 dendrites. *Science* 268:297–300

Stafstrom CE, Schwindt PC, Crill WE. 1984. Cable properties of layer V neurons from cat sensorimotor cortex in vitro. *J. Neurophysiol.* 52:278–89

Stern P, Edwards FA, Sakmann B. 1992. Fast and slow components of unitary EPSCs on stellate cells elicited by focal stimulation in slices of rat visual cortex. *J. Physiol.* 449:247–78

Storm JF. 1990. Potassium currents in hippocampal pyramidal cells. *Prog. Brain Res.* 83:161–87

Stratford K, Mason A, Larkman AU, Major G, Jack JJ. 1989. The modelling of pyramidal neurons in the visual cortex. In *The Computing Neuron*, ed. R Durbin, C Miall, G Mitchison, pp. 296–321. Wokingham, UK: Addison-Wesley

Stuart G, Spruston N. 1998. Determinants of voltage attenuation in neocortical pyramidal neuron dendrites. *J. Neurosci.* 18:3501–10

Stuart G, Spruston N, Sakmann B, Häusser M. 1997. Action potential initiation and backpropagation in neurons of the mammalian CNS. *Trends Neurosci.* 20:125–31

Stuart GJ, Sakmann B. 1994. Active propagation of somatic action potentials into neocortical pyramidal cell dendrites. *Nature* 367:69–72

Stuart GJ, Spruston N, Häusser M. 1999. *Dendrites*. New York: Oxford Univ. Press.

Suzuki T, Kodama S, Hoshino C, Izumi T, Miyakawa H. 2008. A plateau potential mediated by the activation of extrasynaptic NMDA receptors in rat hippocampal CA1 pyramidal neurons. *Eur. J. Neurosci.* 28:521–34

Takahashi N, Kitamura K, Matsuo N, Mayford M, Kano M, et al. 2012. Locally synchronized synaptic inputs. *Science* 335:353–56

Tateno T, Harsch A, Robinson HP. 2004. Threshold firing frequency-current relationships of neurons in rat somatosensory cortex: type 1 and type 2 dynamics. *J. Neurophysiol.* 92:2283–94

Trussell LO, Fischbach GD. 1989. Glutamate receptor desensitization and its role in synaptic transmission. *Neuron* 3:209–18

Varga Z, Jia H, Sakmann B, Konnerth A. 2011. Dendritic coding of multiple sensory inputs in single cortical neurons in vivo. *Proc. Natl. Acad. Sci. USA* 108:15420–25

Vyklický L Jr, Benveniste M, Mayer ML. 1990. Modulation of *N*-methyl-D-aspartic acid receptor desensitization by glycine in mouse cultured hippocampal neurones. *J. Physiol.* 428:313–31

Waters J, Helmchen F. 2006. Background synaptic activity is sparse in neocortex. *J. Neurosci.* 26:8267–77

Wei DS, Mei YA, Bagal A, Kao JP, Thompson SM, Tang CM. 2001. Compartmentalized and binary behavior of terminal dendrites in hippocampal pyramidal neurons. *Science* 293:2272–75

Wilent WB, Contreras D. 2005. Stimulus-dependent changes in spike threshold enhance feature selectivity in rat barrel cortex neurons. *J. Neurosci.* 25:2983–91

Williams SR. 2004. Spatial compartmentalization and functional impact of conductance in pyramidal neurons. *Nat. Neurosci.* 7:961–67

Williams SR, Stuart GJ. 1999. Mechanisms and consequences of action potential burst firing in rat neocortical pyramidal neurons. *J. Physiol.* 521:467–82

Williams SR, Stuart GJ. 2000. Site independence of EPSP time course is mediated by dendritic I-h in neocortical pyramidal neurons. *J. Neurophysiol.* 83:3177–82

Williams SR, Stuart GJ. 2002. Dependence of EPSP efficacy on synapse location in neocortical pyramidal neurons. *Science* 295:1907–10

Williams SR, Stuart GJ. 2003. Role of dendritic synapse location in the control of action potential output. *Trends Neurosci.* 26:147–54

Wong RKS, Prince DA, Basbaum AI. 1979. Intra-dendritic recordings from hippocampal neurons. *Proc. Natl. Acad. Sci. USA* 76:986–90

Xu NL, Harnett MT, Huber D, O'Connor DH, Svoboda K, Magee JC. 2012. Nonlinear dendritic integration of sensory and motor input during an active sensing task. *Nature* 492:247–51

Yamada M, Inanobe A, Kurachi Y. 1998. G protein regulation of potassium ion channels. *Pharmacol. Rev.* 50:723–60

Yu Y, Shu Y, McCormick DA. 2008. Cortical action potential backpropagation explains spike threshold variability and rapid-onset kinetics. *J. Neurosci.* 28:7260–72

Yuan H, Geballe MT, Hansen KB, Traynelis SF. 2008. Structure and function of the NMDA receptor. In *Structural and Functional Organization of the Synapse*, ed. JW Hell, MD Ehlers, pp. 289–316. New York: Springer Sci.+Bus. Media

Yuste R, Gutnick MJ, Saar D, Delaney KR, Tank DW. 1994. Ca^{2+} accumulations in dendrites of neocortical pyramidal neurons: an apical band and evidence for two functional compartments. *Neuron* 13:23–43

Zhang S, Trussell LO. 1994. Voltage clamp analysis of excitatory synaptic transmission in the avian nucleus magnocellularis. *J. Physiol.* 480(Pt. 1):123–36

Zhu JJ. 2000. Maturation of layer 5 neocortical pyramidal neurons: amplifying salient layer 1 and layer 4 inputs by Ca^{2+} action potentials in adult rat tuft dendrites. *J. Physiol.* 526(Pt. 3):571–87